NanoAnalysis
An International Journal
Available online at: www.jnanoanalysis.net or www.jnanoanalysis.com

Investigation of Products Distribution In Fischer-Tropsch Synthesis By Nano-sized Iron-based Catalyst

Ali Mohajeri*, Yahya Zamani, Laleh Shirazi

Gas Research Division, Research Institute of Petroleum Industry (RIPI), National Iranian Oil Company; West Blvd., Near Azadi Sports Complex P.O.BOX 14665-137, Tehran, Iran

Abstract

Nano-sized iron-based catalyst was prepared by the micro-emulsion method. The composition of the final nano-sized iron catalyst, in term of the atomic ratio contains: 100Fe/4Cu/2Ce. Experimental techniques of XRD, BET, TEM and TPR were used to study the phase, structure and morphology of the catalyst. Fischer-Tropsch Synthesis (FTS) reaction test was performed in a fixed bed reactor at pressure of 17 bars, temperature of 270-310°C with H_2/CO ratio and GHSV 2 $nl.h^{-1}.gCat^{-1}$, respectively. The temperature of the system as a key parameter was changed and its effect on the selectivity and reaction rate was analysed. The results show that the rate of both reactions including of FTS and Water-Gas Shift (WGS) are increased by increasing temperature. For this condition, CO conversion also increased up to 89.1%.

Keywords: Nanoparticles, Iron catalyst, catalyst characterization, Fischer–Tropsch Synthesis, Products distribution.

1. Introduction

The synthesis of liquid fuels from syngas via Fischer-Tropsch synthesis (FTS) is one of the most important processes to solve the shortage of transport fuels [1–3]. In the FTS process, the conversion of syngas over a catalyst is one of the most pivotal steps. Consequently, choosing a suitable catalyst is very important. Iron catalysts are commonly used because of their low costs in comparison to other active metals. Iron-based catalysts have been used as commercial catalysts for FTS to produce a wide range of paraffin and olefin products, ranging from methane to high molecular weight waxes [4-6].

FT synthesis has been successfully commercialized to produce fuel from coal and natural gas [7]. Because

---

* Corresponding author Tel. : + 98 21 48252090 ; fax : +98 21 44739716 E-mail address: mohajeria@ripi.ir

the reserves of coal and natural gas are richer than those of crude oil [8], FT synthesis can supply plentiful liquid fuels for the world in longer times than petroleum refining.

Alkali-promoted iron catalysts have been applied industrially for the Fischer–Tropsch synthesis for many years [9]. These catalysts have a high water–gas shift activity and high selectivity for olefins and appear to be stable when synthesis gas with a high H_2/CO ratio is converted [10-12] to the liquid hydrocarbons. Iron catalysts are often promoted with Cu, which increases the rate of reduction, enabling a lower reduction temperature [10]. According to Anderson [11], the distribution for *n*-paraffins can be described by the Anderson–Schulz–Flory (ASF) equation (1) :

$$m_n = (1- \alpha)\, \alpha^{n-1} \quad (1)$$

where the growth probability factor α is independent of n. m_n is the mole fraction of a hydrocarbon with chain length of n.

The process conditions as well as the catalyst characteristics influence the product selectivity [13,14]. Although extensive research has been carried out on the effect of potassium promoter on the structure of iron catalyst [15], the study of operating conditions including temperature as an important variable is scarce. An increase in reaction temperature results in a shift toward products with a lower carbon number on iron [16], ruthenium [17], and cobalt [17] catalysts. Donnelly and Satterfield [16], and Anderson [11] observed an increase of the olefin-to-paraffin ratio with increasing temperature on potassium-promoted precipitated iron catalysts. However, Dictor and Bell [18] reported a decrease of the olefin selectivity with increasing temperature for unalkalized iron oxide powders. One of the effective parameters on product selectivity and catalyst activity is the reaction temperature. If the temperature is raised above an optimum limit, there would be the deactivation of the catalyst and coke formation. In this work, the activity of Fe-Cu-Ce catalyst is considered to determine products distribution at the temperature range of 270 to 310 ^{0}C.

2. Experimental

2.1. Catalyst Preparation

Nano-structure iron catalysts were prepared by the microemulsion method. A water solution of metal precursors, $FeCl_3·6H_2O$ was added to a mixture of 2-Propanol and chloroform and sodium dodecyl sulfate (SDS) as a surfactant. Soduim hydroxide aqueous was added as precipitating agent and stirred for 4 hour. The solid was recovered by centrifugation and washed thoroughly with distilled water, ethanol and acetone. Finally, the samples were dried overnight at 120 °C, and subsequently calcined in air at 400 °C for 3 h. Nanostructured Cerium and copper oxides were prepared like nanostructured Fe. At the next step, they were mixed together. The promoted catalysts were dried at 110 ^{o}C for 16 h and calcined at 400 °C for 3 h in air [19-21]. The catalyst was pressed into pellet, crushed and sieved to obtain particles with 30-40 mesh.

2.2. Catalyst characterization

BET Surface area and pore volume of the catalysts were determined by N_2 physisorption using a Micromeritics ASAP 3020 automated system. A 0.3 g catalyst sample was degassed in the system at 100 °C for 1 h and then at 300 ^{o}C for 2 h prior to analysis. The analysis was done using N_2 adsorption at -196 ^{o}C. Average particle size of the calcined powders was measured by LEO 912AB TEM. XRD spectra of fresh catalyst were conducted with a Philips PW1840 X-ray diffractometer with monochromatized Cu (Kα) radiation to determine the iron phases. Temperature programmed reduction (TPR) profiles of the calcined catalysts were recorded using a Micromeritics TPD-TPR 290 system.

2.3. Reactor system and operating procedure

As shown in Figure 1, the catalytic reaction experiments were conducted in a fixed-bed stainless steel reactor. Flow rate of inlet gases and reactor pressure were controlled by electronic mass flow and pressure controllers, respectively. A four heating zone furnace with temperature controller and indicator supplied the required reaction heat.

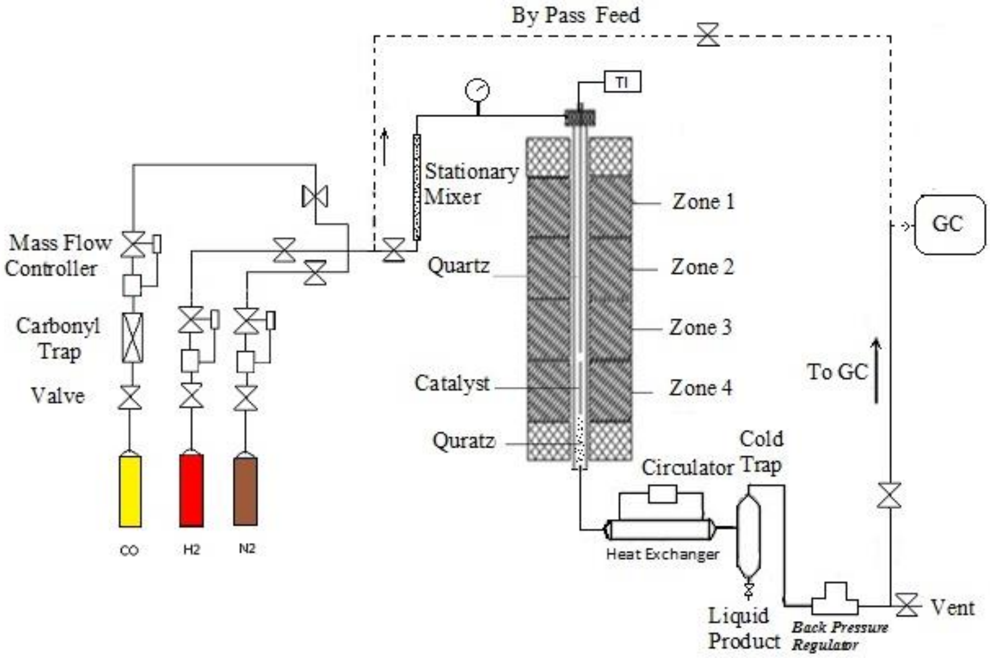

Figure 1. Catalyst test system

The reactor was loaded by 1 g of catalyst. The catalyst was reduced in a %10 H_2/N_2 flow for 3h at 400 ^oC. The catalyst activation was followed in a stream of synthesis gas with H_2/CO of 1 and SV of $1.5 nl.h^{-1}.gCat^{-1}$ for 24 h in atmospheric pressure and temperature of 270 °C. Following the activation process, the reactor pressure and temperature were raised to 17 bar and 270 up to 310 ^oC , respectively and the reaction initiated in synthesis gas stream with H_2/CO =1 and GHSV= $2.8 nl.h^{-1}.gCat^{-1}$.

2.3. Product analysis

The products were analysed by two gas chromatographs (Varian CP 3800). The first one includes was two packed columns connected to two thermal conductivity detectors (TCD) which were used for analysing H_2 ,CO, CO_2 , CH_4 and other non-condensable gases. The other one with a petrocol Tm DH100 fused silica capillary column attached to a flame ionization detector (FID) for analysing hydrocarbon liquid products [22-24]. The activities and product selectivities were assessed after 72 h from start of the run time.

3. Results and discussion

Table 1 shows the BET results for catalyst surface area. By adding Cerium, the BET surface area and pore volume in the catalyst decreased as Cerium promoted the aggregation of the catalyst crystallites and blocked up the pore volume of the catalyst.

X-ray diffraction patterns of the prepared catalyst (Figure 2) show narrow and high intensity peaks, suggesting that the sample is highly crystalline of small particle sizes and that the most abundant phase is Fe_2O_3.

Table 1 : Surface area and pore volume of the catalyst

Catalyst	BET Surface area (m^2/g)	Pore Volume (cm^3/g)
100Fe/4Cu/2Ce	46.3	0.26

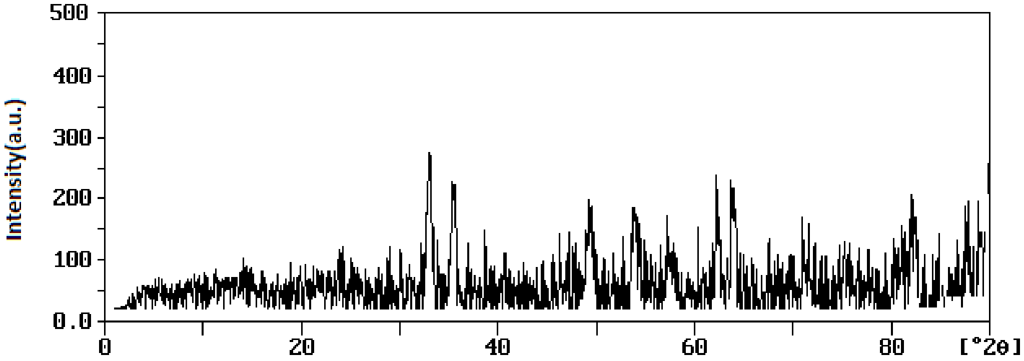

Figure 2. XRD spectra of the fresh 100Fe/4Cu/2Ce catalyst

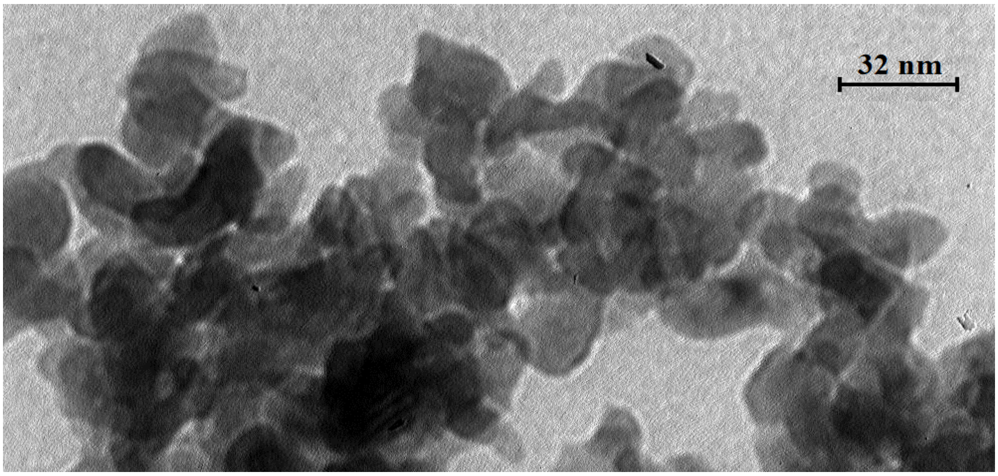

Figure 3. TEM micrograph of 100Fe/4Cu/2Ce catalyst

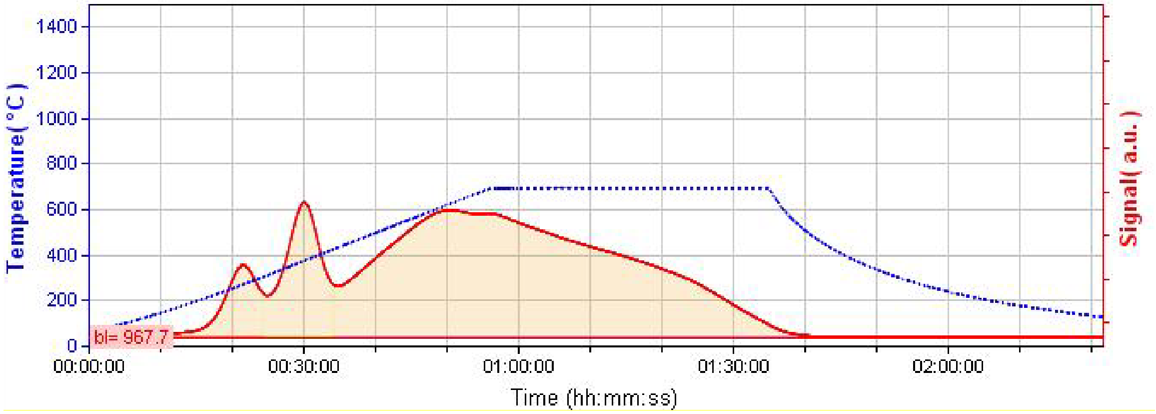

Figure 4. H_2-TPR profile of the catalyst

Table 2. R_{FTS} and R_{WGS} of the catalyst

	270 (°C)	**290 (°C)**	**310 (°C)**
R_{CO2} (mmolCO$_2$/gCat.h)	0.0121	0.0168	0.0243
R_{FTS} (mmolCH$_2$/gCat.h)	0.0217	0.0314	0.0373

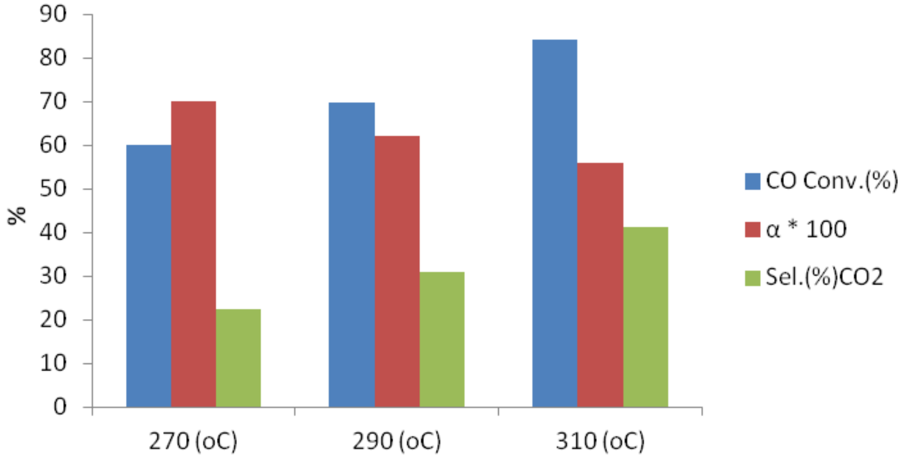

Figure 5. Temperature effect on CO conversion, chain growth probability and CO_2 Selectivity

The morphology of catalyst was illustrated by TEM images that are shown in figure 3. Although TEM revealed that the diameter of nanoparticle was in the range of 10 to 40 nm. Figure 4 shows the H_2-TPR profile of the nano-sized iron catalyst. This curve determines the reduction behaviour of the catalyst. The first stage is ascribed to the transformations of CuO to Cu; the second stage is attributed to the transformation of Fe_2O_3 to Fe_3O_4 whereas the third stage represents the transformation of Fe_3O_4 to Fe [25,26]. Table 2 shows the rates of FTS and WGS at different temperatures. Figure 5 shows CO conversion, chain growth probability and CO_2 selectivity in different temperatures.

In this figure, it can be seen that with increasing temperature from 270 to 310 °C, the CO conversion gradually increased from 60.1% to 84.2%. It seems that the increasing temperature has a lot of influence on CO_2 selectivity, which increases from 22.3% to 41.2% in the temperature range of 270 to 310 °C. In fact the increase of temperature enhances the catalyst activity. Table 3 shows product selectivity of the catalyst at different temperatures. According to this figure, the selectivity of light hydrocarbons including methane and C_2 to C_4 is improved by increasing temperature of the system.

Table 3. Product selectivity of the catalyst in different temperatures (The reaction is occurred at: a time of reaction 62 h, 1.7MPa, H_2/CO = 1 and SV= 2.8 nl.gCat $^{-1}$. h^{-1}.)

Compounds	**270 (°C)**	**290 (°C)**	**310 (°C)**
CH_4	6.8	12.6	19.3
C_2-C_4	35.5	39.8	43.6
C_5-C_{12}	34.1	26.4	21.5
C_{13}-C_{19}	14.9	12.9	7.7
C_{19}^+	8.7	8.3	7.9

On the other hand, the Selectivity of higher hydrocarbons (Selectivity to oxygenates was negligible (<3%) in all cases) decrease with increasing temperature. All results imply that the rate of hydrogenation reactions is enhanced while temperature is increased.

In Table 3, it can be seen that with increasing temperature from 270 to 310 °C, the CO conversion gradually increased from 60.1% to 84. 3%. It seems that increasing temperature has little influence on CO_2 selectivity, which remains at about 41.2% in the temperature range of 270–310 °C. With increasing temperature, the H_2/CO usage ratio was kept constant at 1.

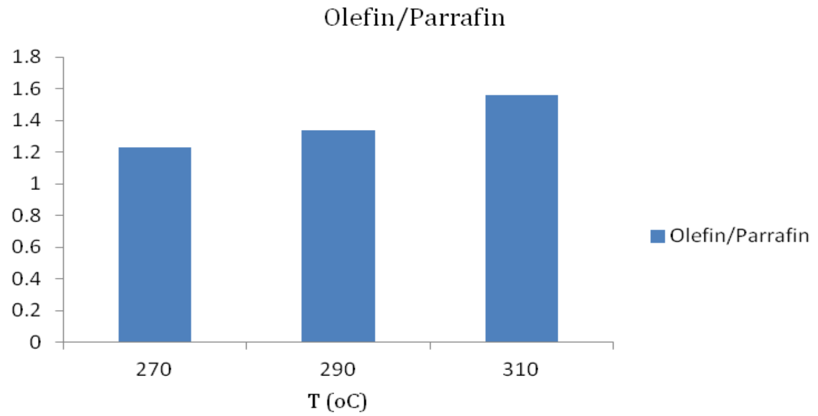

Figure 6. Olefin to paraffin ratio of the catalyst in different temperatures

The methane selectivity increased with increasing temperature. From Table 3, it can also be seen that the selectivity to light alkenes is relatively high, and increased with increasing temperature except for C_5^+, which decreased from 57.7% to 37.1%.

Figure 6 shows Olefin to paraffin ratio of the catalyst in different temperatures. This figure shows that Olefin to paraffin ratio of the catalyst is enhanced while temperature is increased. However, reaction conditions influence the product selectivity.

4. Conclusion

Cerium-promoted nano iron catalyst was studied using different characterization techniques. The effect of temperature on the Fischer–Tropsch synthesis activity and products selectivity was investigated in a fixed-bed reactor. It was observed that the activity and methane selectivity increased while C_5^+ selectivity decreased with increasing temperature. The changes in the catalytic performances can be attributed to the effect of temperature on H_2 adsorption, which significantly affect the FTS performances of the catalysts. The activity of 100 Fe/4Cu/2Ce catalyst has the best performance in FTS at 290 °C.

Acknowledgements

We are grateful to the Research and Development of National Iranian Oil Company (NIOC) for the financial support.

References

1. M.E. Dry, Appl. Catal. A, 189, 185 (1999).
2. H. Schulz, Appl. Catal. A 186, 3 (1999).
3. S. H. Kang, Koo, A.R. Kim, D.H. Lee, J.H. Ryu, Y.D. Yoo, J.W Bae., Fuel Proces. Techno., 109, 141(2013).
4. S. Li, G.D. Meitzner, E. Iglesia, J. Phys. Chem. B 105, 5743 (2001).
5. G.P. Van der Laan, A. A. C. M. Beenackers, Catal. Rev. Sci. Eng. 41, 255(1999).
6. R.L. Espinoza, A.P. Steynberg, B. Jager, A.C. Vosloo, Appl. Catal. A, 186, 13 (1999).
7. A.P. Steynberg, R.L. Espinoza, B. Jager, A.C. Vosloo, Appl. Catal. A, 186, 41(1999).
8. H.H. Schobert, C. Song, Fuel, 81, 15(2002).
9. M. Feyzi, F. Jafari, J. Fuel Chem. Techno., 40, 550 (2012).
10. B. Jager and R. Espinoza, Catal. Today, 23, 17 (1995).
11. R. B. Anderson, " Catalysts for the Fischer–Tropsch Synthesis", Van Nostrand Reinhold, New York, 1956, Vol. 4
12. Y.Zamani ,M.Bakavoli,M.Rahimizadeh,A. Mohajeri S.M.Seyyedi, ,*Chem. Eng. Trans.*,2012,29,847(2012).
13. W.Y. Mao, Q.W. Sun, W.Y. Ying, D.Y. Fang, J. Fuel Chem. Techno, 41, 314(2013).

14. L.A. Cano, M.V Cagnoli, J. F. Bengoa, A.M. Alvarez, S.G. Marchetti, J. Catal., 278, 310(2011).
15. L. Mingsheng and B. H. Davis, Fuel Chem. Division Preprints, 47, 160(2002).
16. T. J. Donnelly and C. N. Satterfield, Appl Catal, 52**,** 93(1989).
17. M. E.Dry, in Catalysis—Science and Technology, Springer-Verlag, New York, 1981, vol.1, 160–255.
18. R. A. Dictor and A. T. Bell, J. Catal, 97**,** 121(1986).
19. Nakhaei Pour, S. Taghipoor, M. Shekarriz, S. M. K. Shahri, Y. Zamani J.Nanosci.Nanotech.,8 , 1(2008).
20. Y. Zamani , M. Bakavoli, M. Rahimizadeh, A. Mohajeri , S. M. Seyedi , Chin. J. Catal. **,** 33, 1119(2012).
21. Y. Zamani,A. Zamaniyan,F.Bahadoran,M.Shojaei,J.Petro.scien.Techno., Inpress(2014).
22. Y. Zamani, S.H. Yousefian, A. N. Pour ,B. Moshtari, F. Bahadoran, S. A. Taheri ,Chem Eng Trans, 21,1045(2010).
23. A. Mohajeri ,Y. Zamani , M. Bakavoli, M. Rahimizadeh, , S. M. Seyedi , J.Petro.scien.Techno., Inpress(2014).
24. N. Pour, S.M. Kamali Shahri, H. R. Bozorgzadeh, Y. Zamani, A. Tavasoli, M. M. Ahmadi , Appl Catal A: Gen, 348, 201(2008).
25. A. Mohajeri , Y.Zamani ,M. Bakavoli, M. Rahimizadeh, , S.M.Seyyedi, ,Petroleum *Research*, Inpress(2014).
26. Y. Jin, A. K. Datye, J. Catal., 196 , 8(2000).